Computer Methods in Biomechanics and Biomedical Engineering
Vol. 15, No. 8, August 2012, 875–884

Taylor & Francis
Taylor & Francis Group

Using topological equivalence to discover stable control parameters in biodynamic systems

Martin L. Tanaka[a,b]* and Shane D. Ross[b1]

[a]*Department of Engineering and Technology, Western Carolina University, 333 Belk, Cullowhee, NC 28723, USA;* [b]*Department of Engineering Science and Mechanics, Virginia Tech, 224 Norris Hall, Blacksburg, VA 24061, USA*

(*Received 13 August 2010; final version received 19 February 2011*)

In order to better understand the mechanisms that contribute to low back pain, researchers have developed mathematical models and simulations. A mathematical model including neuromuscular feedback control is developed for a person balancing on an unstable sitting apparatus, the wobble chair. When the application of a direct method fails to discover appropriate controller gain parameters for the wobble chair, we show how topological equivalence can be used to indirectly identify appropriate parameter values. The solution is found by first transforming the wobble chair into the Acrobot, another member of the same family of topologically equivalent dynamical systems. After finding appropriate gain parameters for the Acrobot, a continuous transformation is performed to convert the Acrobot back to the wobble chair, during which the gain parameters are adjusted to maintain stability. Thus, we demonstrate how topological equivalence can be used to indirectly solve a problem that was difficult to solve directly.

Keywords: stability; spine; Hilbert envelope; solution space; Lyapunov stability; topological equivalence

1. Introduction

Low back pain (LBP) is a common medical condition that affects most people sometime during their life (Kelsey and White 1980; Reeves et al. 2005). In order to better understand the mechanisms that contribute to LBP, researchers have developed mathematical models and simulations (Panjabi 1992; Granata and Wilson 2001; Reeves and Cholewicki 2003; Franklin and Granata 2007; Tanaka and Ross 2009; Tanaka et al. 2009, 2010; Ross et al. 2010). These models generally consist of rigid body segments, springs, dampers and actuators that represent the spine, paraspinal tissue and muscles of the torso. In addition, some models also include neuromuscular control to simulate the system dynamics. Among the many types of controllers that may be used to simulate the neuromuscular control of the spine, one of the simplest and most common is proportional derivative (PD) control (Tan et al. 2002; Knospe 2006). PD control uses two parameters, the proportional gain G_p and the derivative gain G_d to quantify the control behaviour. However, sometimes finding controller gain parameters that produce stable behaviour is difficult when the system is nonlinear, and the set of controller parameters leading to stable behaviour is small.

The goal of this paper is to show how topological equivalence can be used to find controller gain parameters when the use of a direct method fails to yield results. In order to demonstrate this, we will develop a mathematical model of a person balancing on an unstable sitting apparatus, the wobble chair (Cholewicki et al. 2000; Slota et al. 2008; Tanaka et al. 2010). We will show how using a direct approach to find PD control parameters to stabilise the system was not successful (Figure 1). Next, we will demonstrate how topological equivalence can be used to transform the wobble chair into the Acrobot, another member of the same family of topologically equivalent dynamical systems. Controller gain parameters were found for the Acrobot which produce stable system behaviour. With a solution for the Acrobot known, a continuous transformation will be performed to convert the Acrobot back to the wobble chair. During this transformation, the controller gain parameters will be adjusted to maintain stable system behaviour throughout the transformation. Finally, the space of controller parameters is divided into regions leading to stability and instability for both the Acrobot and the wobble chair through the application of the evolution rule and the convergence rate of the Hilbert envelope.

1.1 Topological equivalence

Topological equivalence is a mathematical concept that may be used to characterise dynamical systems. Two dynamical systems are said to be 'topologically equivalent' if the phase portraits are qualitatively similar (Meiss 2007). That is, one portrait can be obtained from the other by a continuous transformation (Figure 2). In mathematics, topological equivalence is a concept within the major area

*Corresponding author. Email: mtanaka@wcu.edu

ISSN 1025-5842 print/ISSN 1476-8259 online

http://dx.doi.org/10.1080/10255842.2011.565413
http://www.tandfonline.com

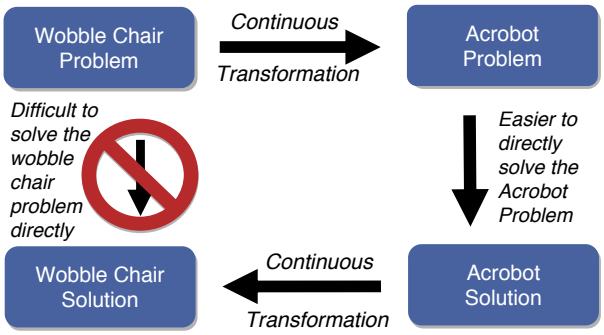

Figure 1. Flow map of paper showing how topological equivalence is exploited using continuous transforms. A difficult problem that cannot generally be solved directly is transformed to an easier problem which is solved, and then transformed back to obtain a solution to the original problem.

of topology, a field of study that is concerned with the preservation of geometric properties of objects under continuous deformation. Simply stated, if an object can be stretched or deformed into another shape without tearing it or gluing parts of it together, then these two objects are topologically equivalent. The classic example is the transformation of a doughnut into a coffee cup (Peterson 1998). Transformations are commonly used to classify both the dynamical systems (e.g. equilibrium stability types and normal forms) (Meiss 2007) and to make seemingly difficult problems easier to solve. In the context of a dynamical system, transformations can be thought of as a change of phase space variables or a change of parameters.

Although topological equivalence is not a new concept, its application to biodynamics appears to be uncommon. A few studies of legged locomotion have used solutions of simpler approximate models as a starting point for more complicated, realistic models (Geyer 2004; Ghigliazza et al. 2005; Seipel 2005, 2006). Our contention is that a more systematic approach of the use of topological equivalence could lead to greater insight into biodynamic problems as well as practical problem-solving ability.

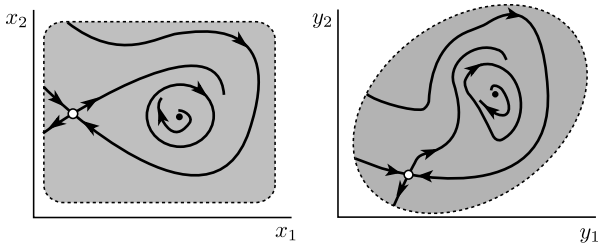

Figure 2. Topological equivalence. Notice that the phase portrait of y can be created through a continuous deformation of x.

2. The planar double pendulum family

2.1 Mathematical model

The unstable sitting apparatus, also known as a wobble chair (Figure 3(a)), is used to study the factors that contribute to spinal instability and LBP (Tanaka and Granata 2007; Lee and Granata 2008; Slota et al. 2008; Tanaka 2008). The seat assembly pivots on a central low-friction ball joint and moves with the lower body. Stabilising springs are positioned to the front, back, left and right of the central ball joint. Moving these springs closer to the centre decreases the restorative moment applied to the seat, thereby increasing task difficulty. During testing, the upper body moves with respect to the lower body pivoting at the lumbar spine. Small movements of the lumbar spine are used to maintain balance. This system is simplified by collecting the upper body components and lower body components to create two rigid body segments (Tanaka et al. 2010).

This two-segment model of the wobble chair is a member of the family of planar double inverted pendulums. Members of the family may differ in mass, mass distribution or segment lengths, but despite these differences in inertial and geometric properties, they all share the same topologically equivalent solutions to the equations of motion. The property of having topologically equivalent phase portraits is reflected in similarities of the equations of motion. Using a Lagrangian approach, the equation of motion for this family is

$$M\ddot{\theta} + C(\theta, \dot{\theta})\dot{\theta} + G(\theta) = \tau, \tag{1}$$

where θ, $\dot{\theta}$ and $\ddot{\theta}$ are the rotation angle, the angular velocity and the angular acceleration vectors, respectively. The matrices **M**, **C** and **G** are defined as

$$\mathbf{M} = \begin{bmatrix} m_1\|\vec{c}_1\|^2 + m_2\left\|\vec{L}_1\right\|^2 + I_1 & m_2\left(R'_{\theta 1}\vec{L}_1\right)\cdot\left(R'_{\theta 2}\vec{c}_2\right) \\ m_2\left(R'_{\theta 1}\vec{L}_1\right)\cdot\left(R'_{\theta 2}\vec{c}_2\right) & m_2\|\vec{c}_2\|^2 + I_2 \end{bmatrix}, \tag{2}$$

$$\mathbf{C} = \begin{bmatrix} 0 & m_2\left(R'_{\theta 1}\vec{L}_1\right)\cdot\left(R''_{\theta 2}\vec{c}_2\right)\dot{\theta}_2 \\ m_2\left(R''_{\theta 1}\vec{L}_1\right)\cdot\left(R'_{\theta 2}\vec{c}_2\right)\dot{\theta}_1 & 0 \end{bmatrix}, \tag{3}$$

$$\mathbf{G} = \begin{bmatrix} m_1\vec{g}\cdot\left(R'_{\theta 1}\vec{c}_1\right) + m_2\vec{g}\cdot\left(R'_{\theta 1}\vec{L}_1\right) \\ m_2\vec{g}\cdot\left(R'_{\theta 2}\vec{c}_2\right) \end{bmatrix}, \tag{4}$$

$$\theta = \begin{bmatrix} \theta_1 \\ \theta_2 \end{bmatrix}, \tag{5}$$

where m_i is the segment mass, $\vec{c}_i$ is the vector from the joint to the segment centre of mass, $\vec{L}_i$ is the segment position vector, I_i is the segment moment of inertia, g is the acceleration of gravity and τ_i is the external torque. The

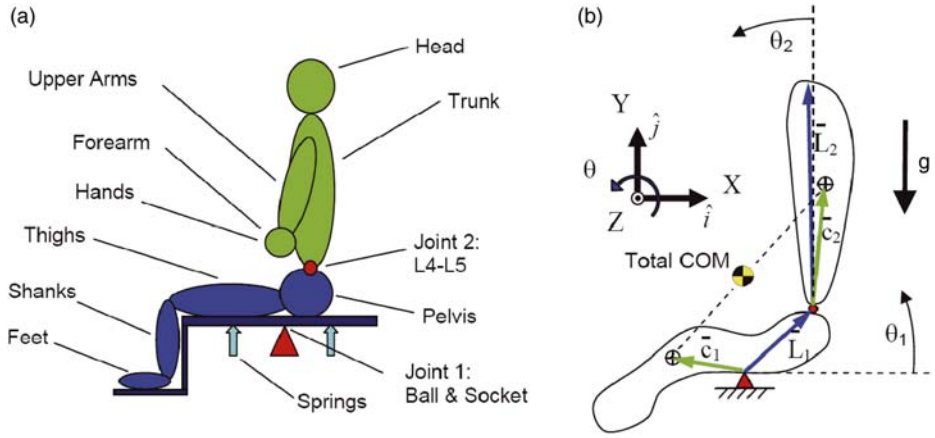

Figure 3. (a) Wobble chair and (b) simplified wobble chair model (Tanaka et al. 2010).

subscript i indicates the segment number, 1 or 2. Parameters $\mathbf{R}'_{\theta i}$ and $\mathbf{R}''_{\theta i}$ are the first and second time derivatives of the rotation matrix,

$$\mathbf{R}_{\theta i} = \begin{bmatrix} \cos\theta_i & -\sin\theta_i \\ \sin\theta_i & \cos\theta_i \end{bmatrix}. \tag{6}$$

The wobble chair is also part of a subset of this family which has control, stiffness and damping between the two segments and no control at the attachment point of the first segment. For this subset,

$$\tau = \begin{bmatrix} \tau_{\mathrm{Spr}} - (\tau_{\mathrm{sk}} + \tau_{\mathrm{sd}} + C_{\mathrm{PD}}) \\ \tau_{\mathrm{sk}} + \tau_{\mathrm{sd}} + C_{\mathrm{PD}} \end{bmatrix}. \tag{7}$$

Compression springs (k_1) at distance d_1 are included in the model ($\tau_{\mathrm{Spr}} = k_1 d^2 \sin\theta_1$) as well as passive torques at the lumbar spine due to elastic stiffness (k_2: with $\tau_{\mathrm{sk}} = k_2(\theta_2 - \theta_1)$) and viscous damping ($k_3$: with $\tau_{\mathrm{sd}} = k_3(\dot{\theta}_2 - \dot{\theta}_1)$). PD control torque, C_{PD}, is applied between the two segments to represent the muscles of the torso that flex or extend the spine. To achieve balance, control torque is applied to cause flexion when the overall centre of mass θ_{COM} deviated to the posterior and extension when θ_{COM} deviated to the anterior. Thus, PD control torque is

$$C_{\mathrm{PD}}(\theta, \dot{\theta}) = G_{\mathrm{d}}\dot{\theta}_{\mathrm{COM}} + \begin{cases} G_{\mathrm{P}}\theta_{\mathrm{COM}}, & \text{if } |\theta| < \theta_{\mathrm{cr}}, \\ \tau_{\mathrm{pmax}}, & \text{otherwise}, \end{cases} \tag{8}$$

where

$$\theta_{\mathrm{COM}} = \arctan\left(\frac{\vec{c}_{\mathrm{COM}} \cdot \hat{j}}{\vec{c}_{\mathrm{COM}} \cdot \hat{i}}\right), \tag{9}$$

$$\vec{c}_{\mathrm{COM}} = \frac{m_1\vec{c}_1 + m_2(\vec{L}_1 + \vec{c}_2)}{m_1 + m_2}, \tag{10}$$

G_{d} is the derivative gain constant, $\theta_{\mathrm{cr}} = \tau_{\mathrm{pmax}}/G_{\mathrm{p}}$ is the smallest angle at which the maximum gain is achieved, G_{p} is the proportional gain constant and τ_{pmax} is the maximum value of proportional torque.

2.2 *Direct determination of stable control parameters*

The Ziegler and Nichols (1942) method is used to manually tune the control system parameters with the goal of obtaining stable system behaviour. When this method is applied, all gain parameters are set to zero and the proportional gain increased until oscillations occur (Atherton 2009). This value of proportional gain is identified as the critical gain. The proportional gain is reduced to half the critical gain value and the derivative gain is then increased. Once generally stable performance is achieved, the system is manually tuned to improve system performance based on observed feedback. However, when this trial and error method is applied to the wobble chair, no stable behaviour is observed for any value of proportional gain attempted. Due to the failure of this method to identify stable gain parameters, an alternative method is attempted as described in Section 3.

3. Continuous transformation between family members

The Acrobot (Murray and Hauser 1991) is a two-segment system which represents a person swinging on a high bar (Figure 4) and its simplified model is a member of the family of planar double pendulums. It is also within the subset of this family that has actuation between the segments, but not at the attachment to the fixed reference. Notice the similarity between the Acrobot and the simplified model of the wobble chair (Figure 3(b)). The only differences are in the magnitudes of the inertial and geometric parameters (Table 1). A key point is the

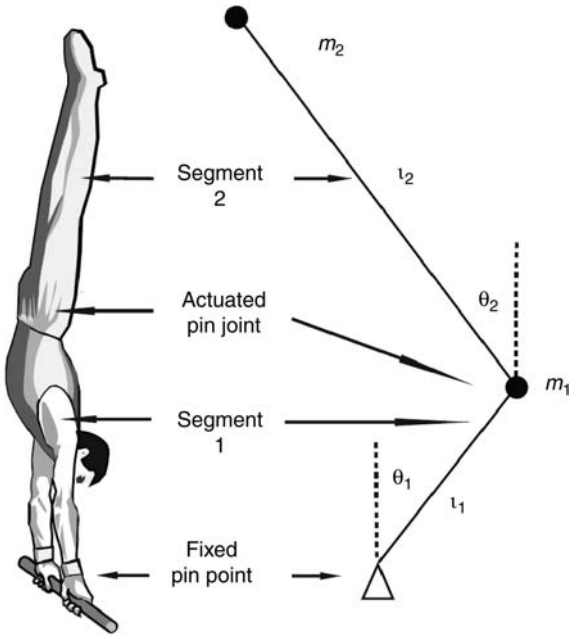

Figure 4. The Acrobot (acrobatic robot) is patterned after a gymnast on a high bar. Actuation occurs only at the middle joint (hip) with the first joint (hands) being free to spin about its axis.

following: it is advantageous to study this better known, simpler and symmetric system in order to gain insight into how to control the wobble chair, which is more complicated and less symmetric, but part of the same dynamical family.

Both the Acrobot and wobble chair are underactuated systems, meaning they posses fewer actuation directions than degrees of freedom (Spong 1995). Murray and Hauser (1991) coined the term 'Acrobot' and were the first to show that this underactuated system was controllable. Since then, others have evaluated the dynamics of the Acrobot (Spong 1995; Boone 1997) and similar dynamical systems (Hou and Luecke 2003). The Acrobot is highly nonlinear with strong coupling between segments. This coupling was used by Spong (1995) to achieve a linear response from the first segment through momentum coupling with the second segment. This resulted in exponential convergence of segment 1. However, the movement of segment 2 was complex since its motion was dictated by the dynamics required to generate the coupling forces needed to control segment 1. Thus, segment 2 could not be controlled for exponential convergence simultaneously with segment 1.

One important property of the Acrobot is the existence of an equilibrium manifold (Murray and Hauser 1991). The manifold exists when the combined centre of mass of the two segments lies directly above the free swinging pin joint. With an appropriate torque at the middle joint, this configuration is able to achieve equilibrium where the two angles, θ_1 and θ_2, are static. The existence of an equilibrium manifold is significant because it indicates that there is a continuum of equilibrium points which exists along the length of the manifold. Thus, stability for the Acrobot (and any member of its family within the subset) may be achieved with more than one combination of θ_1 and θ_2. By topological equivalence, there exists an equilibrium manifold in the wobble chair as well, which was previously unknown and unappreciated.

3.1 Finding stable control parameters for the transformed system

The Ziegler and Nichols method is used to find a proportional gain value which results in stable system behaviour for the Acrobot. Unlike the case when this

Table 1. Model parameters.

Inertial parameters		
	Wobble chair	Acrobot
m_1 (kg)	27.4	8
m_2 (kg)	31.8	8
I_1 (kg m^2)	2.35	0
I_2 (kg m^2)	4.86	0

Geometric parameters (m)						
	Wobble chair			Acrobot		
	x	y	z	x	y	z
L_1	0.1272	0.1580	0	0	0.5	0
L_2	0	0.7179	0	0	1.0	0
c_1	−0.1771	0.0780	0	0	0.5	0
c_2	0	0.2736	0	0	1.0	0

Note: Acrobot parameters from Murray and Hauser (1991).

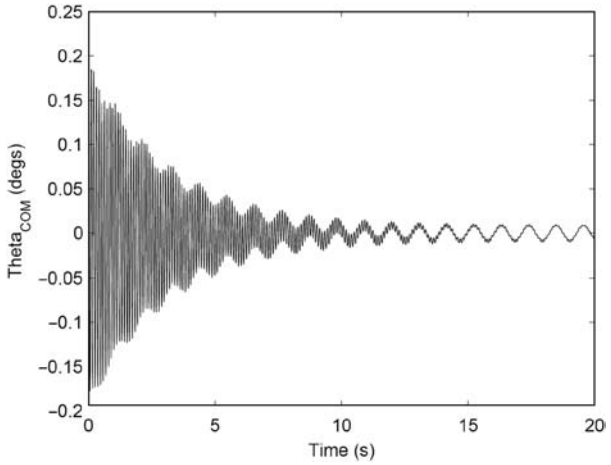

Figure 5. Forward dynamic simulation of the Acrobot showed that the selected PD controller gain parameters drove the centre of mass to near equilibrium ($G_p = 3 \times 10^4$ Nm/rad and $G_d = 6$ Nm/rad s).

method was applied to the wobble chair, stable system behaviour is found as the proportional gain is increased. Derivative gain is added and the system is tuned for adequate performance ($G_p = 3 \times 10^4$ Nm/rad and $G_d = 6$ Nm/rad s). With these parameters, the controller is able to drive θ_{COM} from an initial angle of 1° of upright vertical to within 0.1° with what appears to be exponential convergence (Figure 5). We note that this convergence will be quantified using the Hilbert envelope method described below.

4. Transformation: Acrobot → wobble chair

Beginning with the solution for the Acrobot, stable gain parameters for the wobble chair are found by a gradual transformation. This procedure exploits the fact that for differential dynamical systems, the system solutions vary smoothly and continuously (as opposed to discontinuously) as the system parameters are changed (Meiss 2007). Initially, keeping all other parameters the same, the masses are increased in small steps from the Acrobot values to the wobble chair values ($m_1 = 8 \rightarrow 27.4$ kg; $m_2 = 8 \rightarrow 31.8$ kg). At each step, the proportional and derivative gains are adjusted based on observable system performance. Next, the moments of inertia are changed ($I_1 = 0 \rightarrow 2.35\,\text{kg m}^2$; $I_2 = 0 \rightarrow 4.86\,\text{kg m}^2$) and the PD parameters further refined. Finally, the segment and centre of mass vectors are slowly changed.

In order to gradually transform the geometry, a continuation variable, x, is defined. The variable, x, is used to simultaneously control the magnitude of all geometric parameters of the model including L_1, L_2, c_1 and c_2. For a given value of x, the magnitude of $L_1 = L_{1\,\text{Acrobot}}(x) + L_{1\,\text{WobbleChair}}(100\%-x)$, where $L_{1\,\text{Acrobot}}$ is the value of L_1 for the Acrobot and $L_{1\,\text{WobbleChair}}$ is the value of L_1 for the wobble chair. The other geometric parameters are calculated similarly. During the transformation, the segment vectors and centre of mass vectors (Table 1) are $x\%$ Acrobot and $(100-x)\%$ wobble chair. Thus, by changing the value of x, the model is linearly transformed from one geometric state to the other. Some of the intermediate configurations are shown in Figure 6. As the system was slowly transformed, the controller gain parameters were adjusted to maintain stable system behaviour. After completing the transformation to the family member of interest (wobble chair), convergent behaviour is observed with $G_p = 6 \times 10^6$ Nm/rad and $G_d = 200$ Nm/rad s (Figure 7).

5. Control parameter space partitioned into regions of stability and instability

The previous analysis showed that stable PD gain parameters could be found for both the Acrobot and the wobble chair. However, we still do not understand why the Acrobot is easier to solve than the wobble chair. In order to investigate this, an analysis is conducted to test for stability of these systems over a large range of proportional and derivative gain parameters. A two-dimensional representation of G_p vs. G_d makes up the control space, $C_S = \{(G_p, G_d) \in \Re^2 | G_p \in [0, \infty), G_p \in [0, \infty)\}$. Two methods will be used to evaluate the stability of the system for various combinations of G_p and G_d. The first is the direct calculation of the trajectory using the evolution rule (Bagnoli and Rechtman 1999; Jost 2005; Kami and Ikeda 2009), and the second is the determination of the expansion or contraction of oscillation magnitude using the Hilbert envelope method (Bracewell 2000; Schmid et al. 2004; Amoud et al. 2008). For both methods, an initial condition of $(\theta_1, \theta_2, \dot{\theta}_1, \dot{\theta}_2) = (-2.2°, 1.8°, 0, 0)$ is used to begin each simulation. This initial condition is near, but slightly off the equilibrium manifold. The trajectory is tracked as it evolves under the influence of the controller and the two methods will be used to evaluate if the trajectory is stable or unstable for the given set of control parameters in order to determine the control basin, i.e. the region of control parameters leading to stability (Thompson et al. 1990).

5.1 Calculating the control basin using the evolution rule

Trajectories are calculated by applying the evolution rule that maps the future state of the system based on the current state. Stability is determined by determining if trajectories remain within the neighbourhood of the equilibrium manifold over a finite period of time (15 s). Trajectories begin at the initial location in state space and map out a trajectory as they evolve. Controller gain parameters that produce trajectories which remain close to

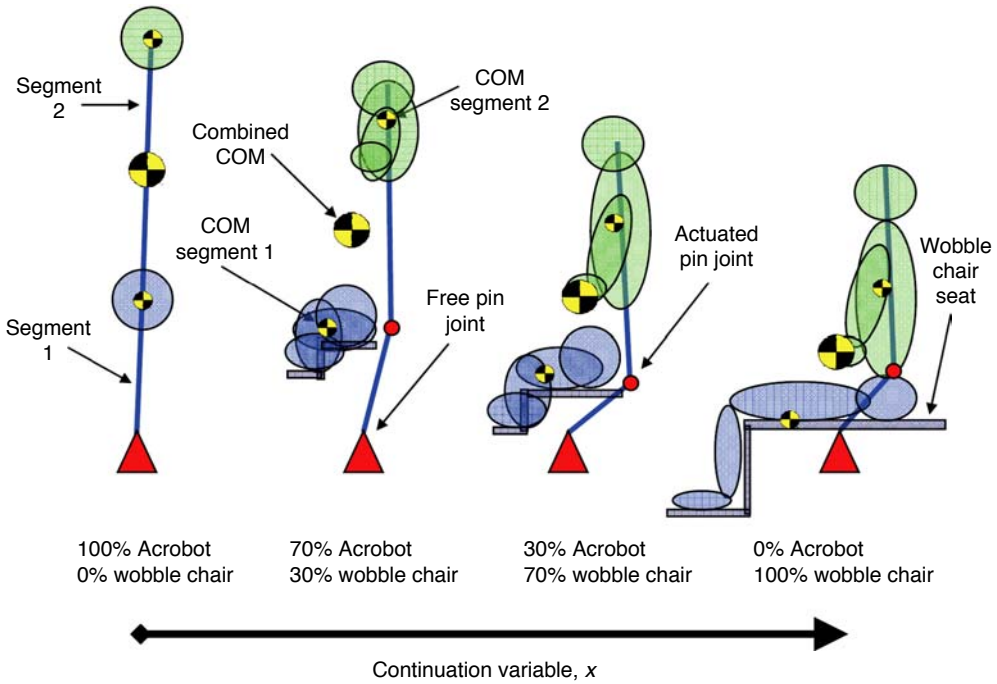

Figure 6. Transformation of the Acrobot to the wobble chair. Increasing the continuation variable, x, causes the geometry to continuously transform from the Acrobot to the wobble chair (four distinct cases are shown). The ground reference for the Acrobot and the wobble chair is located at the tip of the pivot. For the Acrobot, this is the location of the high bar held by the gymnast, and for the wobble chair it is where the central ball joint is attached to the seat.

the equilibrium manifold for the entire evolution time are defined as stable trajectories, whereas those trajectories that exit the neighbourhood are defined as unstable. For this study, the neighbourhood is defined as being within 15° of the equilibrium manifold in configuration space. Trajectories that exit this neighbourhood are stopped.

5.2 *Calculating the control basin using the Hilbert envelope*

Stability of the system is also evaluated by determining whether the amplitude of oscillations are increasing or decreasing. The amplitude of the envelope of the oscillating signal can be determined using a Hilbert transform. Hilbert transforms have been used in electrical communication (Gabor 1946; Wulich 1993), optics (Born and Wolf 1959; Poon and Doh 2007), astronomy (Bracewell 1985; Guillaume 2002) and electromyography (Georgakis et al. 2003), as well as postural stability (Schmid et al. 2004; Amoud et al. 2008). The Hilbert transform of a real function $f(t)$ is defined by Bracewell (2000) as

$$h(t) = \frac{1}{\pi}\int_{-\infty}^{\infty} \frac{f(\tau)}{\tau - t}\,\mathrm{d}\tau, \tag{11}$$

where τ is the time parameter over which the integration is performed. The complex analytical signal is constructed by combining the original signal with its Hilbert transform placed in the imaginary plane,

$$z(t) = f(t) + ih(t). \tag{12}$$

This complex analytical signal may also be expressed as a time-varying phasor,

$$z(t) = a(t)\,\mathrm{e}^{\mathrm{i}\theta(t)}, \tag{13}$$

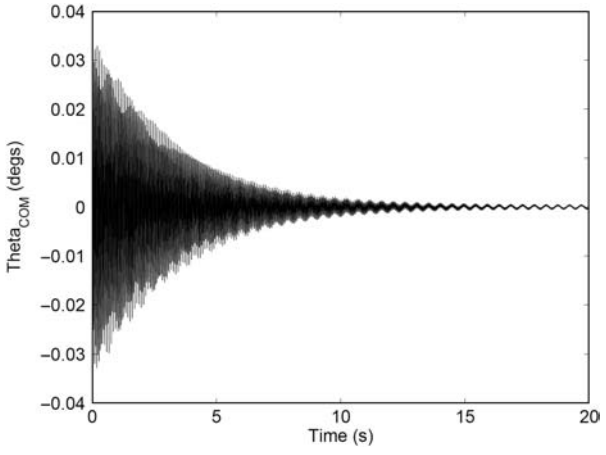

Figure 7. Forward dynamic simulation of the wobble chair showed that the selected PD controller gain parameters drove the centre of mass towards equilibrium manifold ($G_\mathrm{p} = 6 \times 10^6$ Nm/rad and $G_\mathrm{d} = 200$ Nm/rad s).

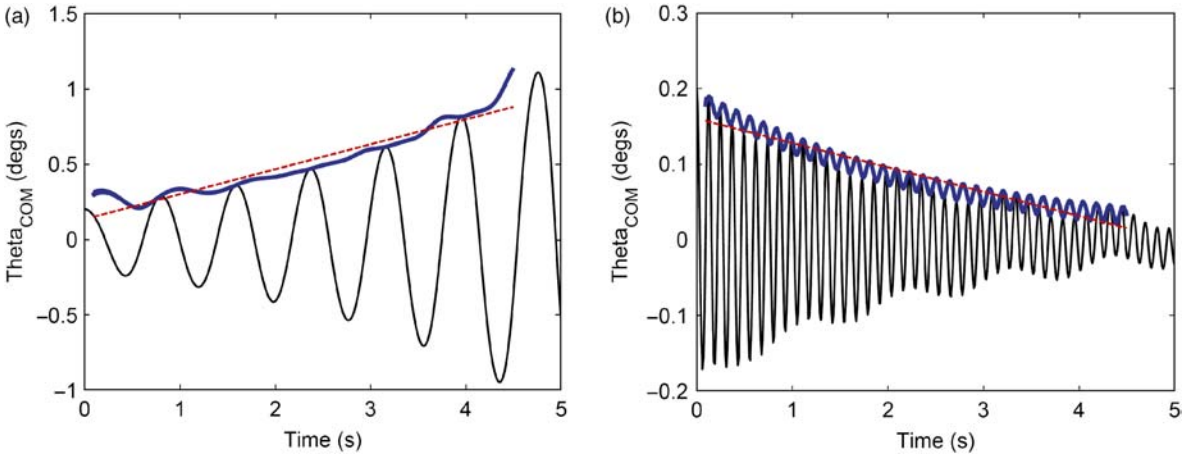

Figure 8. Hilbert transform envelope. (a) The analytical signal (bold line) creates an envelope containing the oscillations of θ_{COM} (solid line). The linear fit to the analytical signal (dashed line) shows a positive slope indicating unstable behaviour ($G_p = 2981$ Nm/rad and $G_d = 20.1$ Nm/rad s). (b) At moderate values of proportional gain and adequate derivative gain, the analytical signal has a negative slope indicating stable behaviour ($G_p = 22{,}026$ Nm/rad and $G_d = 7.39$ Nm/rad s).

where $a(t) = \sqrt{f^2(t) + h^2(t)}$ is the phasor amplitude and $\theta(t)$ is the instantaneous phase (Amoud et al. 2008). The parameter $a(t)$ represents an envelope that approximates the magnitude of the oscillations (Figure 8). In order to determine whether the envelope is converging or diverging, $a(t)$ is fit to a line and the slope is calculated. Positive slopes correlate with an increase in oscillation magnitude indicating unstable behaviour.

5.3 Map of the control basin

Using the above methods, control space is evaluated over a large range ($G_p = [0.3 \times 10^{10}]$, $G_d = [0.3 \times 10^5]$) for the Acrobot (Figure 9(a)) and wobble chair (Figure 9(c)) on a log–log plot of control space. In addition, a 50% Acrobot–50% wobble chair morph is shown (Figure 9(b)). Combinations of controller gain parameters that result in unstable behaviour by both methods are marked with a cross (Figure 8). Points in control space that are identified as stable using the evolution rule but not the Hilbert envelope method are marked with a star. Control space locations that are deemed stable by both methods are marked with a circle. No points were found that were identified as stable using the Hilbert envelope method and unstable using the evolution rule.

The area of control space resulting in stable control behaviour, i.e. the control basin, is observed to shift upwards and to the right as the Acrobot is slowly transformed into the wobble chair. Notice that for the wobble chair, $G_d = 0$ is not in the control basin (both methods). This may explain why stable behaviour is not observed for the wobble chair using the Ziegler and Nichols method. However, when the system is transformed and the method is applied, a solution is found because the Acrobot control basin does contain $G_d = 0$.

There are reasons why the two methods yield different results. For small values of proportional and derivative gain, the controller lacks enough power to stabilise the system. This results in a rapid divergence since the inherently unstable system is essentially not controlled. Under these conditions, both methods indicate instability. However, when the derivative gain is increased to moderate or high levels, the high system damping causes the system to move slowly away from equilibrium. For the relatively short evaluation time of 15 s, the system is able to remain close to the equilibrium point, resulting in a stable assessment using the trajectory evolution method. However, the system is moving away from the equilibrium positions so the envelope is expanding. As a result, the Hilbert envelope method indicates that the system is unstable, a more accurate evaluation.

Stable behaviour is observed for moderate values of proportional and derivative gain. The control basin is observed to be a band from the lower middle moving towards the upper right of control space. When proportional gain is increased beyond this stable region, the system again becomes unstable. This may be due to high controller gains overdriving the system. The observed behaviour was qualitatively similar to the underpowered system with both exhibiting rapid divergence from equilibrium. The similarity in observed behaviour for the under-driven and over-driven systems further supports why appropriate PD parameters were difficult to find.

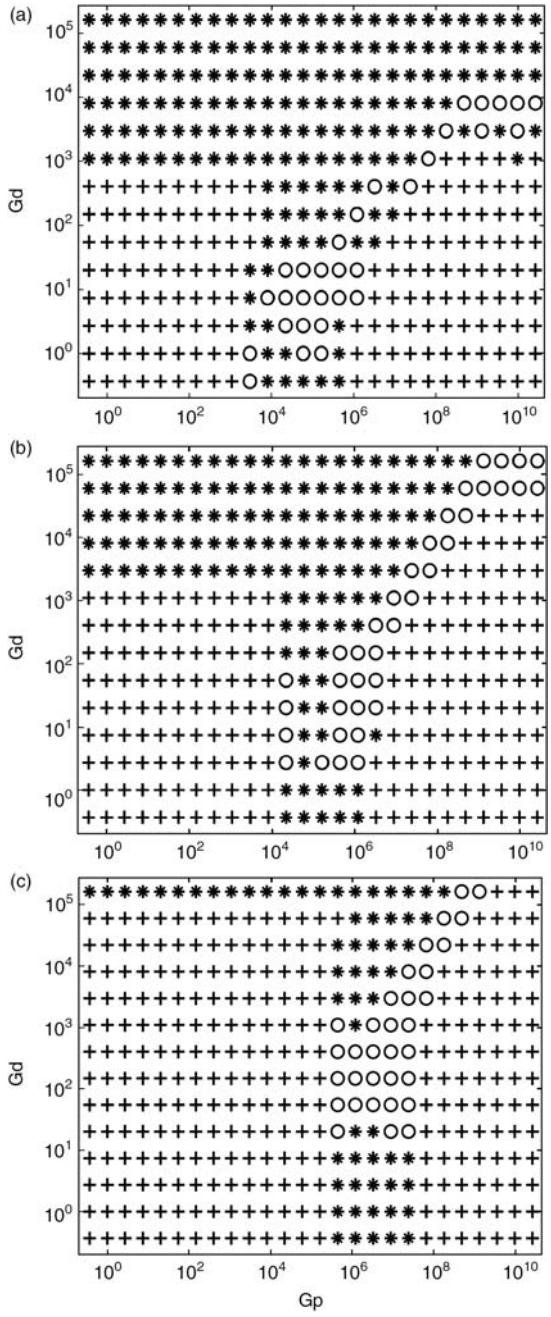

Figure 9. Map of system stability in control space. Simulation results are shown for 100% Acrobot (a), 50% Acrobot and 50% wobble chair (b) and 100% wobble chair (c). For each combination of proportional and derivative gain, a '+' indicates instability using both methods, '∗' indicates stable using the trajectory evolution method and unstable using the Hilbert envelope and 'O' indicates stability using both methods (i.e. the control basin).

6. Conclusions

In this paper, we have shown how a direct approach to find appropriate controller gain parameters for the wobble chair was ineffective and, therefore, introduced an indirect way to solve the problem using topological equivalence. We showed the similarities between members of the same family and how models could be easily transformed between family members. Because these transformations between family members are continuous and the solutions are also continuous, we were able to demonstrate how a solution for an unknown family member could be obtained, given that a solution for one family member was known. This approach allowed us to find appropriate controller gain parameters for the wobble chair model. This mathematical model which included PD feedback control was used to evaluate torso stability and approximate the size of its basin on stability (Tanaka et al. 2010).

We also demonstrated how the slope of the Hilbert envelope could be used to evaluate system stability. This method was found to be more effective than the application of the evolution rule which failed to recognise that slowly diverging systems as unstable. Finally, we used this method to find the regions of control space corresponding to stable behaviour (i.e. the control basin) and compared differences between two family members, the wobble chair and the Acrobot.

Although these methods were applied to torso stability analysis, they may also be useful for studying other types of biodynamic system for which topology can be generated. Possible applications include gait analysis, standing postural sway, tumour growth, population models and cellular signalling. Overall, we believe this approach to be useful for a wide variety of applications where direct solutions have not been successful.

Acknowledgements

The authors express their thanks to Dr Craig A. Woolsey, Associate Professor of Aerospace and Ocean Engineering at Virginia Tech. S.D.R. was supported, in part, by the National Science Foundation, Award 0919088. Partial support for M.L.T. was provided by the Center for Rapid Product Realization at Western Carolina University.

Note

1. Email: sdross@vt.edu

References

Amoud H, Snoussi H, Hewson D, Duchene J. 2008. Univariate and bivariate empirical mode decomposition for postural stability analysis. Eurasip J Adv Signal Process. Available from: <Go to ISI>://000256727800001 doi Artn 657391 doi 10.1155/2008/657391

Atherton D. 2009. Control engineering. Holstebro: Ventus Publishing Aps.

Bagnoli F, Rechtman R. 1999. Synchronization and maximum Lyapunov exponents of cellular automata. Phys Rev E. 59(2):R1307–R1310. Available from: <Go to ISI>://000078779500006

Boone G. 1997. Minimum-time control of the acrobot. Proceedings of the International Conference on Robotics and Automation; April 1997; Albuquerque, NM.

Born M, Wolf E. 1959. Princliples of optics. New York: Pergamon.

Bracewell RN. 1985. Sunspot number series envelope and phase. Aust J Phys. 38(6):1009–1025. Available from: <Go to ISI>://A1985AYX1200022

Bracewell RN. 2000. The Fourier transform and its applications. 3rd ed. Singapore: McGraw-Hill International Editions.

Cholewicki J, Polzhofer GK, Radebold A. 2000. Postural control of trunk during unstable sitting. J Biomech. 33(12):1733–1737. Available from: http://www.ncbi.nlm.nih.gov/entrez/query.fcgi?cmd=Retrieve&db=PubMed&dopt=Citation&list_uids=11006402

Franklin TC, Granata KP. 2007. Role of reflex gain and reflex delay in spinal stability–a dynamic simulation. J Biomech. 40(8):1762–1767. Available from: http://www.ncbi.nlm.nih.gov/entrez/query.fcgi?cmd=Retrieve&db=PubMed&dopt=Citation&list_uids=17054964 doi S0021-9290(06)00296-X [pii] 10.1016/j.jbiomech.2006.08.007

Gabor D. 1946. Theory of communication. J Inst Electr Eng. 93:429–457.

Georgakis A, Stergioulas LK, Giakas G. 2003. Fatigue analysis of the surface EMG signal in isometric constant force contractions using the averaged instantaneous frequency. IEEE Trans Biomed Eng. 50(2):262–265. Available from: <Go to ISI>://000181567400017 Doi 10.1109/Tbme.2002.807641

Geyer H. 2004. Spring-mass running: simple approximate solution and application to gait stability. J Theor Biol. Available doi 10.1016/j.jtbi.2004.08.015

Ghigliazza RM, Altendorfer R, Holmes P, Koditschek D. 2005. A simply stabilized running model. SIAM Rev. 47(3):519. Available doi 10.1137/050626594

Granata KP, Wilson SE. 2001. Trunk posture and spinal stability. Clin Biomech (Bristol, Avon). 16(8):650–659. Available from: http://www.ncbi.nlm.nih.gov/entrez/query.fcgi?cmd=Retrieve&db=PubMed&dopt=Citation&list_uids=11535346 doi S0268-0033(01)00064-X [pii]

Guillaume DW. 2002. A comparison of peak frequency-time plots produced with Hilbert and wavelet transforms. Rev Sci Instrum. 73(1):98–101. Available from: <Go to ISI>://000172906000016

Hou Y, Luecke G. 2003. Control of the tight rope balancing robot. Proceedings of the International Symposium on Intelligent Control; 5–8 October 2003, Houston, TX.

Jost J. 2005. Dynamical systems: examples of complex behaviour. 1st ed. Heidelberg: Springer.

Kami N, Ikeda H. 2009. Topological transition in dynamic complex networks. Phys Rev E. 79(5):056112-1–056112-8. Available from: <Go to ISI>://000266500800018 doi Artn 056112 doi 10.1103/Physreve.79.056112

Kelsey JL, White AA, III. 1980. Epidemiology and impact of low-back pain. Spine. 5(2):133–142. Available from: http://www.ncbi.nlm.nih.gov/entrez/query.fcgi?cmd=Retrieve&db=PubMed&dopt=Citation&list_uids=6446158

Knospe C. 2006. PID control. IEEE Control Syst Mag. 26(1):30–31. Available from: <Go to ISI>://000234766200010

Lee H, Granata KP. 2008. Process stationarity and reliability of trunk postural stability. Clin Biomech (Bristol, Avon). 23(6):735–742. Available from: http://www.ncbi.nlm.nih.gov/entrez/query.fcgi?cmd=Retrieve&db=PubMed&dopt=Citation&list_uids=18304711 doi S0268-0033(08)00026-0 [pii] 10.1016/j.clinbiomech.2008.01.008

Meiss JD. 2007. Differential dynamical systems. Philadelphia, PA: SIAM.

Murray R, Hauser J. 1991. A case study on approximate linearization: the acrobot example. Berkeley, CA: EECS Department, University of California, Berkeley, Technical Report No. UCB/ERL, M91/46. Available from: http://www.eecs.berkeley.edu/Pubs/TechRpts/1991/1760.html and www.cds.caltech.edu/~murray/preprints/erl-M91-46.pdf.

Panjabi MM. 1992. The stabilizing system of the spine. Part I. Function, dysfunction, adaptation, and enhancement. J Spinal Disorders. 5(4):383–389; discussion 397. Available from: http://www.ncbi.nlm.nih.gov/entrez/query.fcgi?cmd=Retrieve&db=PubMed&dopt=Citation&list_uids=1490034

Peterson I. 1998. The mathematical tourist: snapshots of modern mathematics. New York: Holt, Henry & Company, Inc.

Poon TC, Doh KB. 2007. On the theory of optical Hilbert transform for incoherent objects. Opt Express. 15(6):3006–3011. Available from: <Go to ISI>://000245076200027

Reeves NP, Cholewicki J. 2003. Modeling the human lumbar spine for assessing spinal loads, stability, and risk of injury. Crit Rev Biomed Eng. 31(1–2):73–139. Available from: http://www.ncbi.nlm.nih.gov/entrez/query.fcgi?cmd=Retrieve&db=PubMed&dopt=Citation&list_uids=14964352

Reeves NP, Cholewicki J, Milner TE. 2005. Muscle reflex classification of low-back pain. J Electromyogr Kinesiol. 15(1):53–60. Available from: http://www.ncbi.nlm.nih.gov/entrez/query.fcgi?cmd=Retrieve&db=PubMed&dopt=Citation&list_uids=15642653

Ross SD, Tanaka ML, Senatore C. 2010. Detecting dynamical boundaries from kinematic data in biomechanics. Chaos. 20(1):017507. Available from: http://www.ncbi.nlm.nih.gov/entrez/query.fcgi?cmd=Retrieve&db=PubMed&dopt=Citation&list_uids=20370297 doi 10.1063/1.3267043

Schmid M, Conforto S, Bibbo D, D'Alessio T. 2004. Respiration and postural sway: detection of phase synchronizations and interactions. Hum Move Sci. 23(2):105–119. Available from: http://www.sciencedirect.com/science/article/B6V8T-4D0Y5H4-1/2/7657a11179df58f9b072197e7524ee7b

Seipel JE. 2005. Running in three dimensions: analysis of a point-mass sprung-leg model. Int J Robot Res. 24(8):657–674. Available doi 10.1177/0278364905056194

Seipel J. 2006. Three-dimensional translational dynamics and stability of multi-legged runners. Int J Robot Res. 25(9):889–902. Available doi 10.1177/0278364906069045

Slota GP, Granata KP, Madigan ML. 2008. Effects of seated whole-body vibration on postural control of the trunk during unstable seated balance. Clin Biomech (Bristol, Avon). 23(4):381–386. Available from: http://www.ncbi.nlm.nih.gov/entrez/query.fcgi?cmd=Retrieve&db=PubMed&dopt=Citation&list_uids=18093708 doi S0268-0033(07)00260-4 [pii] 10.1016/j.clinbiomech.2007.11.006

Spong MW. 1995. The swing up control problem for the acrobot. IEEE Control Syst Mag. 15(1):49–55. Available from: <Go to ISI>://A1995QE74900010

Tan KK, Huang S, Ferdous R. 2002. Robust self-tuning PID controller for nonlinear systems. J Process Control. 12(7):753–761. Available from: <Go to ISI>://000177016900001 doi Pii S0959-1524(02)00005-7

Tanaka ML. 2008. Biodynamic analysis of human torso stability using finite time Lyapunov exponents. Blacksburg, VA: Virginia Polytechnic Institute and State University (Virginia Tech).

Tanaka ML, Granata KP. 2007. Methods & nonlinear analysis for measuring torso stability. Paper presented at: ASCE 18th Engineering Mechanics Division Conference, Blacksburg, VA.

Tanaka ML, Ross SD. 2009. Separatrices and basins of stability from time series data: an application to biodynamics. Nonlinear Dyn. 58(1):1–21. Available from: http://dx.doi.org/10.1007/s11071-008-9457-9

Tanaka ML, Nussbaum MA, Ross SD. 2009. Evaluation of the threshold of stability for the human spine. J Biomech. 42(8):1017–1022. Available from: http://www.ncbi.nlm.nih.gov/entrez/query.fcgi?cmd=Retrieve&db=PubMed&dopt=Citation&list_uids=19345355 doi S0021-9290(09)00110-9 [pii] 10.1016/j.jbiomech.2009.02.008

Tanaka ML, Ross SD, Nussbaum MA. 2010. Mathematical modeling and simulation of seated stability. J Biomech. 43(5):906–912. Available from: http://www.ncbi.nlm.nih.gov/entrez/query.fcgi?cmd=Retrieve&db=PubMed&dopt=Citation&list_uids=20018288 doi S0021-9290(09)00641-1 [pii] 10.1016/j.jbiomech.2009.11.006

Thompson JMT, Rainey RCT, Soliman MS. 1990. Ship stability-criteria based on chaotic transients from incursive fractals. Philos Trans R Soc A. 332(1624):149–167. Available from: <Go to ISI>://A1990DR70700007

Wulich D. 1993. Hilbert transform of a constant envelope signal using the time-warping technique. Signal Process. 31(1):97–101. Available from: http://www.sciencedirect.com/science/article/B6V18-48TDDFD-1H/2/9edddd6ad66392a0e418fffab4392174

Ziegler JG, Nichols NB. 1942. Optimum settings for automatic controllers. Trans ASME. 64:759–768.